metals

MDPI

Article

# Kinetics of Iron Extraction from Coal Fly Ash by Hydrochloric Acid Leaching

**Dmitry Valeev [1,*], Alexandra Mikhailova [2] and Alexandra Atmadzhidi [1]**

[1] I.P. Bardin Laboratory for Problems of Metallurgy for Complex Ores, A.A. Baikov Institute of Metallurgy and Materials Science, Russian Academy of Sciences, 49, Leninsky Prospect, 119334 Moscow, Russia; alexandra_0492@mail.ru

[2] Laboratory of Crystal Structure Studies, A.A. Baikov Institute of Metallurgy and Materials Science, Russian Academy of Sciences, 49, Leninsky Prospect, 119334 Moscow, Russia; sasham1@mail.ru

* Correspondence: dmvaleev@yandex.ru; Tel.: +7-905-781-66-67

Received: 13 June 2018; Accepted: 29 June 2018; Published: 10 July 2018


**Abstract:** Iron contained in coal fly ash of the Ekibastuz power station is distributed between magnetite and hematite. XRD data showed that ~80 wt % of iron is contained in magnetite and ~20 wt % in hematite. The leaching of iron from CFA by HCl was studied. It was determined that leaching efficiency increased with the increase in hydrochloric acid concentration and temperature. The maximum iron extraction efficiency was 52%. Aluminum is contained in the mullite and was practically not leached. The maximum aluminum extraction efficiency was 3.7%. The kinetics investigation showed that the process of iron leaching was controlled by chemical reaction and diffusion process steps, with an activation energy of 33.25 kJ·mol$^{-1}$. The aluminum leaching process is controlled by a diffusion process step with an activation energy of 19.89 kJ·mol$^{-1}$. The reaction order of hydrochloric acid is determined to be 0.9 and 0.23 for iron and aluminum, respectively.

**Keywords:** coal fly ash; hydrochloric acid; leaching; hematite; magnetite; kinetics

## 1. Introduction

Annually, more than 123 million tons of solid fuel are burnt in Russia in thermal power plants. At the same time, ~25 million tons of coal fly ash (CFA) are formed with only 2 million tons per year being re-processed. Ash dumps occupy large areas within urban land and CFA is transported with high consumption of water (from 10 to 100 m$^3$/t), while the adjoining territories are contaminated, making them unsuitable for economic use. Construction and operation of ash dumps demand considerable investment, leading to increases in the working cost of electrical power [1,2].

Coal fly ash contains up to 30% aluminum oxide, making this type of raw material an attractive alternative to bauxites for alumina production [3–6]. High content of silicon dioxide in ash makes it impossible to use standard alkaline technologies because of significant losses of sodium hydroxide at the processing stage of coal fly ash leaching [7–9]. Accordingly, in recent years, acid methods of processing of high-silica aluminum raw materials have been actively developed [10–13]. However, the use of sulfuric acid can lead to calcium sulfate coating on the surface of ash particles; this prevents interaction between aluminum and sulfate ions, and the application of a fluoride method is accompanied by poisonous emissions of ammonia and fluorine [14–16]. The hydrochloric acid method has a number of advantages compared with the use of other acids:

- low solubility of silicon dioxide in HCl [17];
- possibility of selective crystallization $AlCl_3 \cdot 6H_2O$ [18–20];
- industrially-mastered technology of catching of HCl, i.e., receiving hydrochloric acid for reuse in the course of raw material leaching [21].

In addition to oxides of aluminum and silicon, CFA may contain up to 10% of iron oxide, which can be removed using a wet magnetic separation. However, iron in ash can be presented not only as a magnetite mineral, but also as hematite, which has no magnetic properties and remains in the non-magnetic fraction of ash. It results in chloride-aluminum solutions which are contaminated with iron ions at the subsequent stage of pressure acid leaching [22,23]. There are a number of studies on preliminary processing of bauxite by low concentration hydrochloric acid for removal of unintended impurities: iron oxides, and carbonates of calcium and magnesium [24–29]. This approach is very promising in relation to coal fly ash, since the main alumina mineral, mullite, has low solubility in HCl, and losses of aluminum in this process will be minimum [30]. An aqueous solution of $FeCl_3$ can be recycled by spray pyrolysis at 600 °C. Spheres of α-$Fe_2O_3$ received by this method, can be used as pigments [31–34].

The purpose of the paper were to removing iron oxides and study kinetics and mechanism of interaction of CFA with hydrochloric acid in the range of temperatures of 25–100 °C.

## 2. Materials and Methods

The ash samples were collected from State district power station No. 1 (SDPS-1) located in Ekibastuz, Republic of Kazakhstan. The chemical composition of ash is presented in Table 1.

**Table 1.** Chemical composition of coal fly ash of Ekibastuz's SDPS-1, the Republic of Kazakhstan.

| Composition | $SiO_2$ | $Al_2O_3$ | $Fe_2O_3$ | $TiO_2$ | $K_2O$ | CaO | MgO | MnO | $Na_2O$ | $P_2O_5$ | Loss on Ignition |
|---|---|---|---|---|---|---|---|---|---|---|---|
| Concentration, wt % | 57.1 | 31.3 | 5.31 | 1.30 | 0.41 | 1.78 | 0.65 | 0.09 | 0.42 | 0.33 | 1.31 |

Hydrochloric acid (36.5%, GR ACS) produced by SIGMATEK LLC was used as leaching reagent.

Iron leaching from ash was carried out in the glass flat-bottomed flask of 200 mL installed on a heated magnetic stir bar (US-1500S, ULAB, Moscow, Russia). The experiments were carried out at ambient pressure, 25–100 °C, 5–20% HCl concentration, and over 15–60 min. The ash sample weight was 10 g, with a solid-to-liquid ratio (S:L) of 1 to 10. Upon completion of the experiment, the pulp slurry was cooled and filtered by vacuum filtration. The solids were washed with deionized water and dried at 105 °C for 2 h.

Iron and aluminum extraction rate in solution was calculated according to Equation (1).

$$\eta = [Me_1 \times V / Me_2] \times 100\ \% \quad (1)$$

where $Me_1$ is the content of iron or aluminum in solution after leaching (g/L); $V$ is solution volume after filtration (L); and $Me_2$ is the content of iron or aluminum in the feed ash (g/L). An inductively coupled plasma-atomic emission spectrometer ICAP 6300 DUO (Thermo, Waltham, MA, USA) was used for the chemical analysis of solid and liquid samples.

The X-ray diffraction analysis of feed ash and its magnetic part was carried out using an Ultima IV diffractometer (Rigaku, Tokyo, Japan) in Cu-Kα; radiation in the range of angles 2θ 10–100° at 0.02° intervals. Operating mode of the X-ray source was set at 40 kW/30 mA. In the course of grinding, about 20 wt % content of silica gel was added to the study samples to reduce the preferential grain orientation (texture). The quantitative and qualitative structure of samples were defined using the PDXL (Rigaku) program.

The morphology of the ash particles was examined using an EVO LS 10 (Carl Zeiss, Oberkochen, Germany) and Vega 3 (Tescan, Brno, Czech Republic) scanning electron microscope.

## 3. Results and Discussion

### *3.1. Characterization of the Coal Fly Ash*

As shown in Table 1, the major components of ash are oxides of silicon, aluminum, and iron. According to the X-ray diffraction analysis (Figure 1a), CFA consists of mullite ($3Al_2O_3 \cdot 2SiO_2$), and quartz ($SiO_2$). The X-ray diffraction showed a large amorphous ring which, with the low content of iron oxides in ash, impeded the definition of the main minerals of iron. Hence, a wet magnetic separation of CFA was carried out. The obtained magnetic fraction, besides mullite and quartz, contained magnetite ($Fe_3O_4$) and hematite ($Fe_2O_3$) (Figure 1b). The quantitative analysis of phases showed that magnetite comprises ~80 wt %, and hematite ~20 wt % iron.

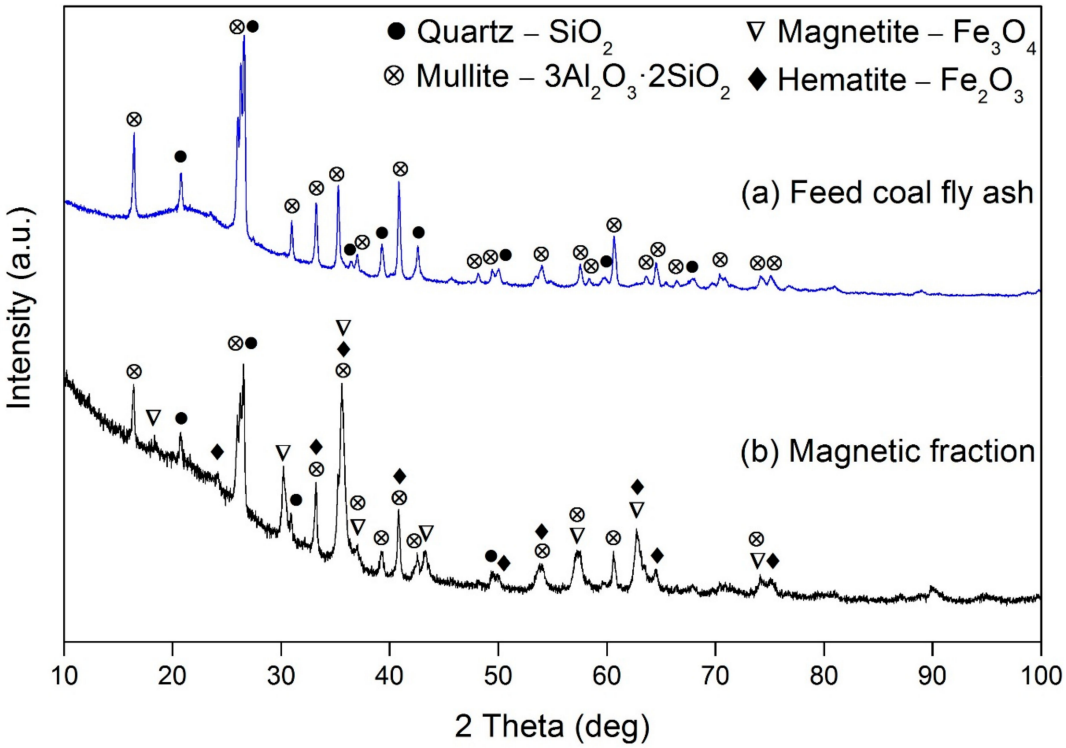


**Figure 1.** XRD patterns of coal fly ash from Ekibastuz's SDPS-1, the Republic of Kazakhstan: (**a**) feed ash; (**b**) magnetic fraction of ash.

SEM images of the CFA studied are shown in Figure 2. Aluminosilicate are composed of irregular and spherical particles. Iron in the ash is composed only of spherical particles with a size of 5 to 150 μm (Figure 2a–c). The surface of these spheres is composed of octahedral particles of magnetite. As shown in Figure 2d, the individual crystals range in size from 200 nm to 2 μm. Crystals can create stick shaped agglomerates of up to 4 μm in length (Figure 2e).

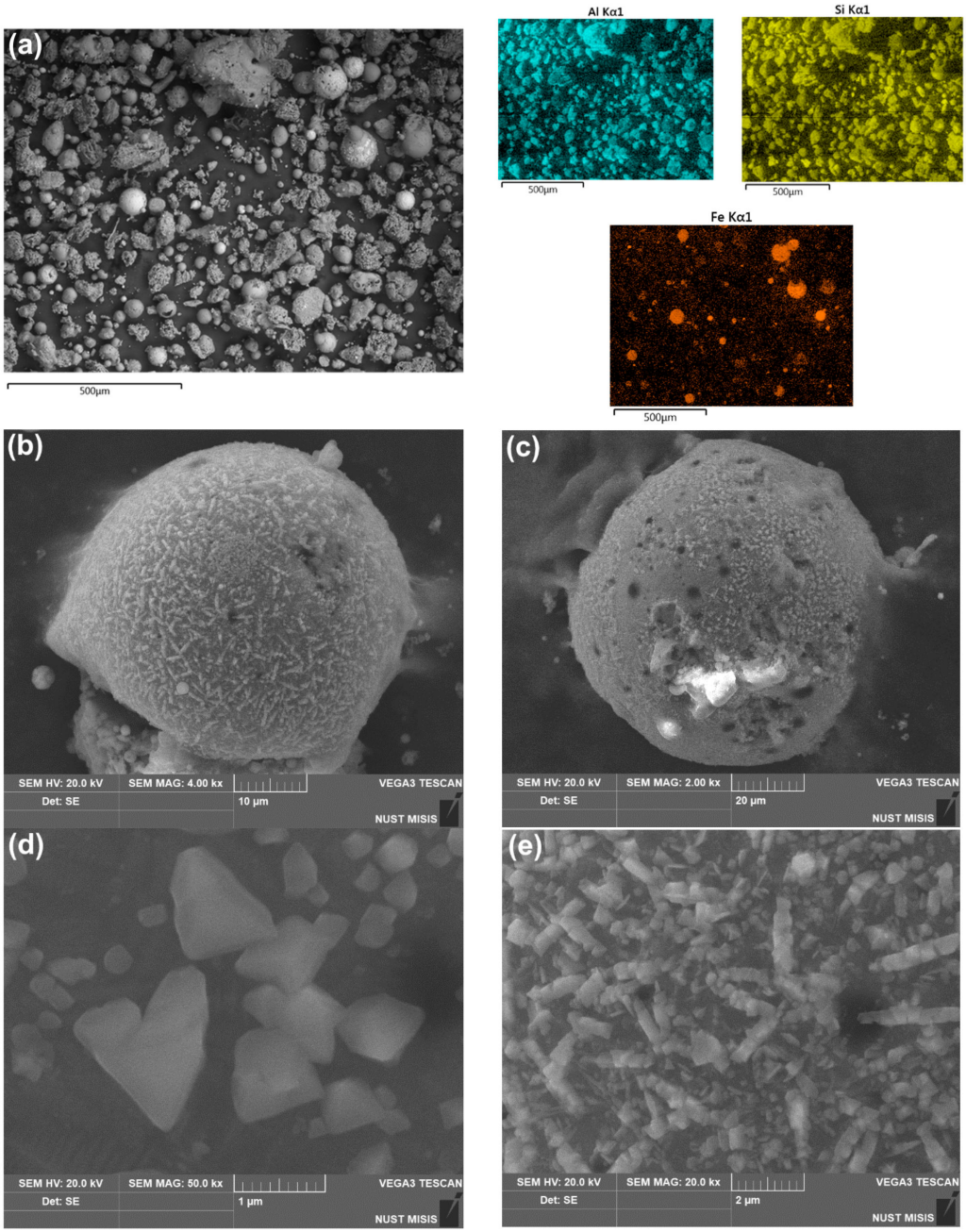


**Figure 2.** SEM images of the CFA samples: (**a**) particles of feed ash (the mapping shows distribution of aluminum, silicon and iron), (**b**,**c**) spherical particles with magnetite on the surface, (**d**) individual octahedral crystals of magnetite, (**e**) stick shaped agglomerates of magnetite.

### *3.2. CFA Leaching by Hydrochloric Acid*

On the basis of XRD data, it is possible to conclude that reactions of ash with hydrochloric acid can be written as:

$$Fe_2O_{3(s)} + 6HCl_{(l)} = 2FeCl_{3(aq)} + 3H_2O_{(l)} \quad (2)$$

$$Fe_3O_{4(s)} + 8HCl_{(l)} = FeCl_{2(aq)} + 2FeCl_{3(aq)} + 4H_2O_{(l)} \quad (3)$$

$$3Al_2O_3 \cdot 2SiO_{2(s)} + 18HCl_{(l)} = 6AlCl_{3(aq)} + 2SiO_{2(s)} + 9H_2O_{(l)} \quad (4)$$

Besides $FeCl_3$, iron chlorides with valency(II) can also be formed in accordance with Equation (3) [35,36].

Figure 3 shows the effect of influence temperature, HCl concentration, and time on CFA leaching. Temperature had the greatest impact on the iron extraction process. Iron extration efficiency at 25 °C did not exceed 5%, but after the temperature was increased to 100 °C, extration efficiency increased to 52% (Figure 3a). At low concentrations of HCl, extration efficiency did not exceed 12%; the dissolution of Fe became faster at 20% HCl (Figure 3b). It should be noted that leaching duration did not have a substantial impact on extration efficiency, regardless of temperature and hydrochloric acid concentration. Losses of aluminum in both cases did not exceed 4% (Figure 3c,d). The experimental errors for iron extractions were ±2%, and ±0.2% for aluminum extractions.

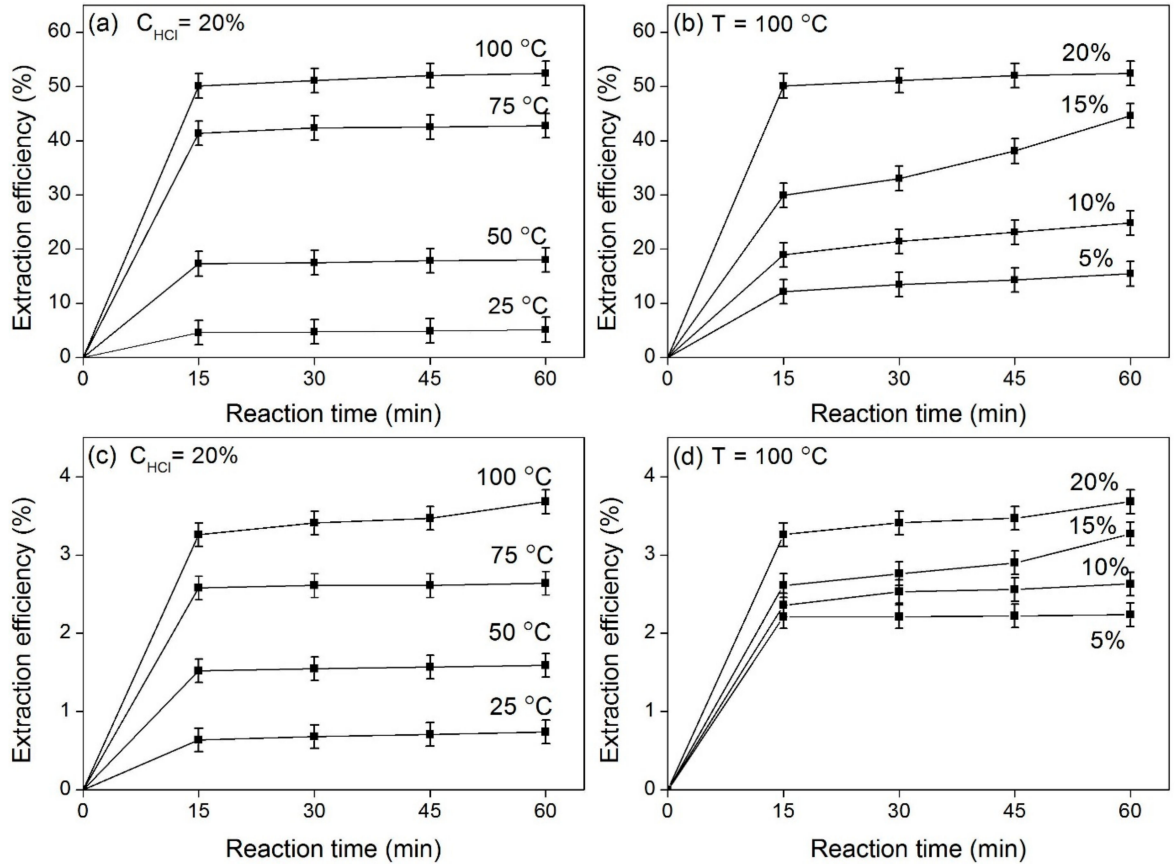


**Figure 3.** Effect of temperature, HCl concentration and time on CFA leaching at S:L = 1:10, $\omega_{\text{stir bar}}$ = 300 rpm: (**a**,**b**) iron extraction efficiency, (**c**,**d**) aluminum extraction efficiency.

### *3.3. Kinetic Study of Fe and Al Leaching in HCl Solutions*

The process of iron and aluminum extraction with hydrochloric acid can be described as the function depending on temperature and concentration of the reacting agents:

$$W = f(T, C) = k\, C_{HCl}{}^{n} \quad (5)$$

where $C$ is hydrochloric acid concentration; $n$ is reaction order with respect to this component; and $k$ is reaction kinetic constant.

Dependence of speed constant on temperature is expressed by the Arrhenius Equation:

$$k = A \cdot \exp(-E_a / RT) \quad (6)$$

where $A$ is the pre-exponential factor characterizing the frequency of reacting molecules collisions; $E_a$ is the activation energy; and $R$ is the universal gas constant: 8.31 J/K mol.

Kinetic characteristics were defined by analysis. For stabilization of the solid's surface, the secant method at the minimum values of extraction rate was used [37]. Hence, the supposition was made that at the same extraction rate, the specific surface of solids at various temperatures and acid concentration was virtually identical. We used a logarithm of tangent slope values constructed to points of intersection of a plane at leaching kinetic curves corresponding to certain values of temperature and concentration of HCl. By this method, we obtained values for the creation of dependences of lnk–1/T and lnk–lnC (Figure 4).

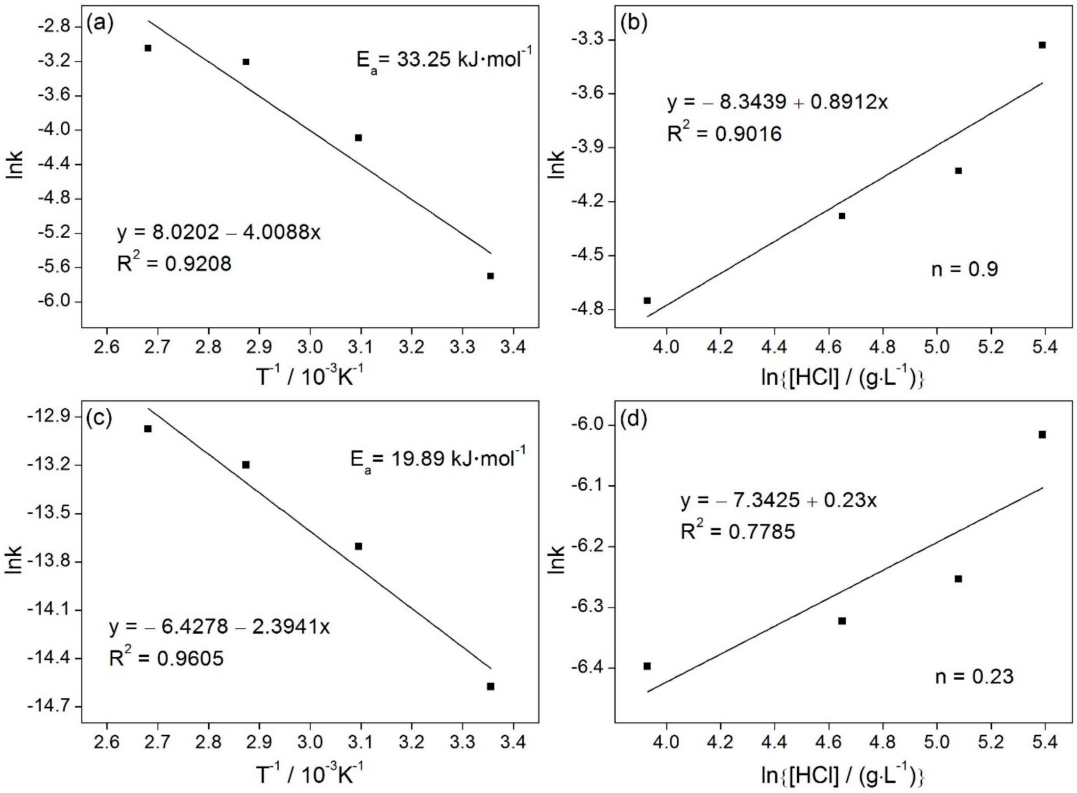


**Figure 4.** Relationship between lnk/$T^{-1}$ and lnk/ln[HCl] during leaching process: (**a**,**b**) for iron, (**c**,**d**) for aluminum.

Diffusion control processes generally have low activation energy values (5–20 kJ·mol$^{-1}$). Chemical reactions have activation energies of more than 45 kJ·mol$^{-1}$. Mixed control of diffusion processes and chemical reactions have activation energies between 25–40 kJ·mol$^{-1}$ [38]. The activation energy of iron leaching was determined to be 33.25 kJ·mol$^{-1}$, meaning that the iron leaching process is controlled by surface chemical reaction and diffusion control processes (Figure 4a). Figure 4b shows the plots of natural logarithms of the apparent rate constant (lnk) versus the natural logarithm of the HCl concentration (ln[HCl]). The results of iron leaching for the reaction order with respect to HCl concentration can be obtained. From Figure 4b, it can be seen that the reaction order for iron leaching was 0.9. The kinetic equation for the effect of temperature and hydrochloric acid concentration on iron leaching rate can be obtained by Equation (7).

$$W_{\mathrm{Fe}} = 3.05 \times 10^3 \times C_{\mathrm{HCl}}{}^{0.9} \times e^{-33252/RT} \quad (7)$$

The activation energy of aluminum leaching was determined to be 19.89 kJ·mol$^{-1}$, meaning that the aluminum leaching process is controlled by diffusion control (Figure 4c). From Figure 4d, it can be seen that the reaction order for aluminum leaching was 0.23. The kinetic equation for the effect

of temperature and hydrochloric acid concentration on aluminum leaching rate can be obtained by Equation (8):

$$W_{Al} = 3.08 \times 10^{-3} \times C_{HCl}{}^{0.23} \times e^{-19895/RT} \quad (8)$$

The mechanism of dissolution of magnetite consists of two stages. In the first stage, iron is dissolved from magnetite crystals on the surface of spherical ash particles. In this stage, the process is limited by the chemical reaction. In the second stage, iron leaching from structure of aluminosilicate occurs. In this stage, the process is limited by diffusion control. As shown in Figure 5a, about 50% of iron located on the surface of the spherical particles was leached. The mapping data in Figure 5b shows that iron was uniformly distributed in the structure of a spherical aluminosilicate particle. The silica substantially complicates the access of the acid to the iron in aluminosilicate.

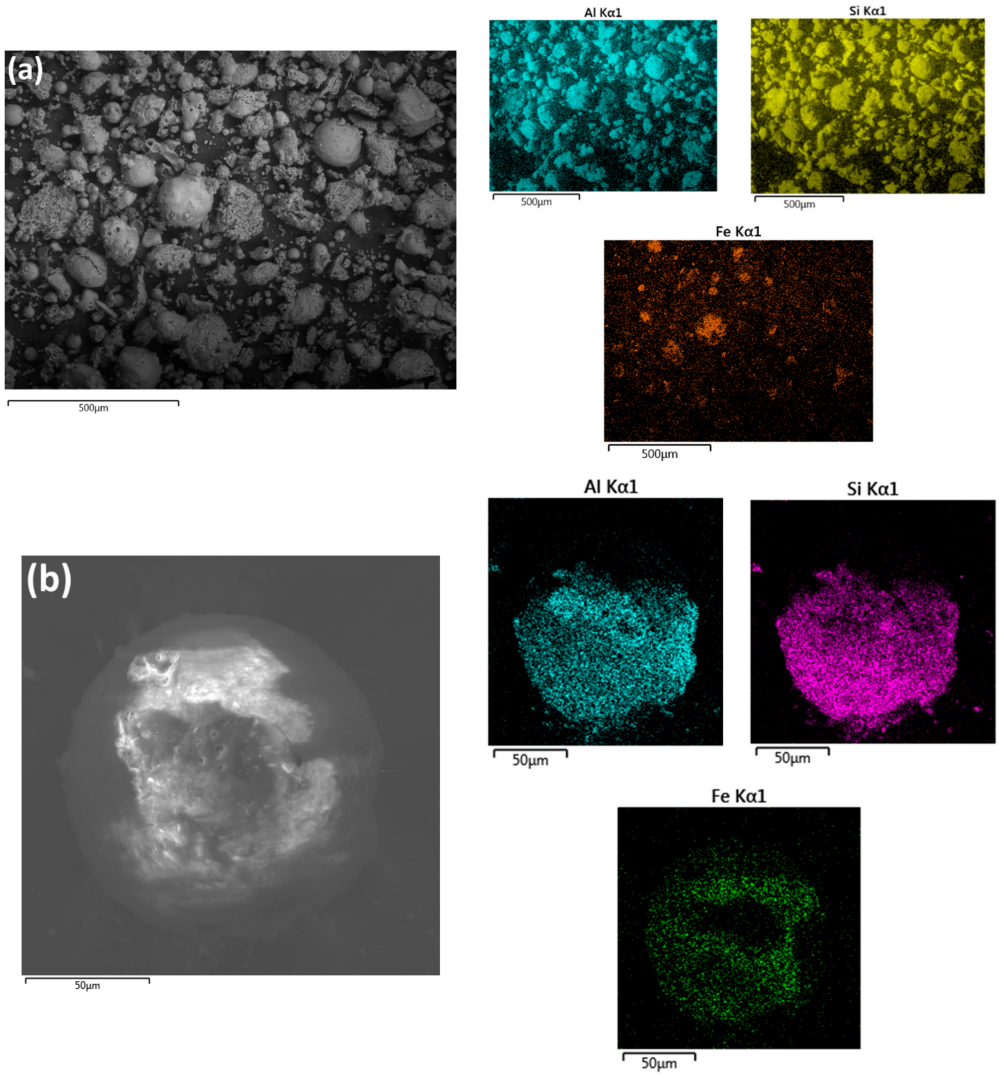


**Figure 5.** SEM images of the CFA samples: (**a**) particles of CFA after leaching by hydrochloric acid at $T$ = 100 °C, $C_{HCl}$ = 220 g/L, S:L = 1:10 and τ = 60 min (the mapping shows distribution of aluminum, silicon and iron), (**b**) spherical particle of CFA (the mapping shows distribution of aluminum, silicon and iron).

## 4. Conclusions

The effects of temperature and HCl concentration on the acid leaching of CFA from Ekibastuz's SDPS-1 were investigated. The maximum iron extraction efficiency was 52%, which was obtained at

$T$ = 100 °C, $C_{HCl}$ = 220 g/L, S:L = 1:10. Losses of aluminum under these conditions did not exceed 4%. Under experimental data, the activation energy and the reaction order of hydrochloric acid were determined to be 33.25 kJ·mol$^{-1}$, 0.9 for iron and 19.89 kJ·mol$^{-1}$, 0.23 for aluminum. The kinetics study showed that the iron leaching process is controlled by chemical reaction and the diffusion process steps. The aluminum leaching process appears to be controlled by the diffusion process step.

**Author Contributions:** D.V. and A.A. designed the research, performed the experiments and analyzed the data. A.M. provided the analysis tools and performed the characterization. D.V. wrote the article.

**Acknowledgments:** The work was carried out in accordance by Russian government state task for basic research No. 007-00129-18-00.

**Conflicts of Interest:** The authors declare no conflict of interest.

## References

1. World Energy Council (WEC). *World Energy Resources*; World Energy Council: London, UK, 2016; p. 1028.
2. Ryabov, Y.V.; Delitsyn, L.M.; Ezhova, N.N.; Lavrinenko, A.A. PAV-2 conditioning agent application efficiency in flotation of unburned carbon from coal-fired power plants fly ash. *Obogashchenie Rud* **2018**, 43–49. [CrossRef]
3. Shemi, A.; Mpana, R.N.; Ndlovu, S.; van Dyk, L.D.; Sibanda, V.; Seepe, L. Alternative techniques for extracting alumina from coal fly ash. *Miner. Eng.* **2012**, *34*, 30–37. [CrossRef]
4. Yao, Z.T.; Xia, M.S.; Sarker, P.K.; Chen, T. A review of the alumina recovery from coal fly ash, with a focus in China. *Fuel* **2014**, *120*, 74–85. [CrossRef]
5. Ding, J.; Ma, S.; Shen, S.; Xie, Z.; Zheng, S.; Zhang, Y. Research and industrialization progress of recovering alumina from fly ash: A concise review. *Waste Manag.* **2017**, *60*, 375–387. [CrossRef] [PubMed]
6. Sun, L.; Luo, K.; Fan, J.; Lu, H. Experimental study of extracting alumina from coal fly ash using fluidized beds at high temperature. *Fuel* **2017**, *199*, 22–27. [CrossRef]
7. Lu, M.; Chang, Y.; Chen, L. Kinetics of desilification pretreatment from high-aluminium coal fly ash in alkaline medium under pressure. *Chem. Res. Chin. Univ.* **2017**, *33*, 282–286. [CrossRef]
8. Jiang, Z.Q.; Yang, J.; Ma, H.W.; Wang, L.; Ma, X. Reaction behaviour of $Al_2O_3$ $SiO_2$ in high alumina coal fly ash during alkali hydrothermal process. *Trans. Nonferr. Met. Soc. China* **2015**, *25*, 2065–2072. [CrossRef]
9. Wang, R.C.; Zhai, Y.C.; Ning, Z.Q.; Ma, P.H. Kinetics of $SiO_2$ leaching from $Al_2O_3$ extracted slag of fly ash with sodium hydroxide solution. *Trans. Nonferr. Met. Soc. China* **2014**, *24*, 1928–1936. [CrossRef]
10. Sangita, S.; Nayak, N.; Panda, C.R. Extraction of aluminium as aluminium sulphate from thermal power plant fly ashes. *Trans. Nonferr. Met. Soc. China* **2017**, *27*, 2082–2089. [CrossRef]
11. Seidel, A.; Zimmels, Y. Mechanism and kinetics of aluminum and iron leaching from coal fly ash by sulfuric acid. *Chem. Eng. Sci.* **1998**, *53*, 3835–3852. [CrossRef]
12. Wu, C.Y.; Yu, H.F.; Zhang, H.F. Extraction of aluminum by pressure acid-leaching method from coal fly ash. *Trans. Nonferr. Met. Soc. China* **2012**, *22*, 2282–2288. [CrossRef]
13. Xu, D.; Li, H.; Bao, W.; Wang, C. A new process of extracting alumina from high-alumina coal fly ash in $NH_4HSO_4$ + $H_2SO_4$ mixed solution. *Hydrometallurgy* **2016**, *165*, 336–344. [CrossRef]
14. Seidel, A.; Sluszny, A.; Shelef, G.; Zimmels, Y. Self inhibition of aluminum leaching from coal fly ash by sulfuric acid. *Chem. Eng. J.* **1999**, *72*, 195–207. [CrossRef]
15. Tripathy, A.K.; Sarangi, C.K.; Tripathy, B.C.; Sanjay, K.; Bhattacharya, I.N.; Mahapatra, B.K.; Behera, P.K.; Satpathy, B.K. Aluminium recovery from NALCO fly ash by acid digestion in the presence of fluoride ion. *Int. J. Miner. Process.* **2015**, *138*, 44–48. [CrossRef]
16. Cheng, F.; Cui, L.; Miller, J.D.; Wang, X. Aluminum leaching from calcined coal waste using hydrochloric acid solution. *Miner. Process. Extr. Metall. Rev.* **2012**, *33*, 391–403. [CrossRef]
17. Smirnov, A.; Kibartas, D.; Senyuta, A.; Panov, A. *Miniplant Tests of HCl Technology of Alumina Production*; Springer: Berlin/Heidelberg, Germany, 2018; pp. 3–8.
18. Cui, L.; Cheng, F.; Zhou, J. Preparation of high purity $AlCl_3 \cdot 6H_2O$ crystals from coal mining waste based on iron(III) removal using undiluted ionic liquids. *Sep. Purif. Technol.* **2016**, *167*, 45–54. [CrossRef]
19. Guo, Y.; Lv, H.; Yang, X.; Cheng, F. $AlCl_3 \cdot 6H_2O$ recovery from the acid leaching liquor of coal gangue by using concentrated hydrochloric inpouring. *Sep. Purif. Technol.* **2015**, *151*, 117–183. [CrossRef]

20. Zhang, N.; Yang, Y.; Wang, Z.; Shi, Z.; Gao, B.; Hu, X.; Tao, W.; Liu, F.; Yu, J. Study on the thermal decomposition of aluminium chloride hexahydrate. *Can. Metall. Q.* **2018**, *57*, 235–244. [CrossRef]
21. Al-Othman, A.; Demopoulos, G.P. Gypsum crystallization and hydrochloric acid regeneration by reaction of calcium chloride solution with sulfuric acid. *Hydrometallurgy* **2009**, *96*, 95–102. [CrossRef]
22. Singh, R.; Singh, L.; Singh, S.V. Beneficiation of iron and aluminium oxides from fly ash at lab scale. *Int. J. Miner. Process.* **2015**, *145*, 32–37. [CrossRef]
23. Haider, U.; Bittnar, Z.; Kopecky, L.; Šmilauer, V.; Pokorny, J.; Zaleska, M.; Prošek, Z.; Hrbek, V. Determining the role of individual fly ash particles in influencing the variation in the overall physical, morphological, and chemical properties of fly ash. *Acta Polytech.* **2016**, *56*, 265–282. [CrossRef]
24. Reddy, B.; Mishra, S.; Banerjee, G. Kinetics of leaching of a gibbsitic bauxite with hydrochloric acid. *Hydrometallurgy* **1999**, *51*, 131–138. [CrossRef]
25. Zhao, A.C.; Liu, Y.; Zhang, T.A.; Lü, G.Z.; Dou, Z.H. Thermodynamics study on leaching process of gibbsitic bauxite by hydrochloric acid. *Trans. Nonferr. Met. Soc. China* **2013**, *23*, 266–270. [CrossRef]
26. Zhao, A.; Zhang, T.A.; Lv, G.; Tian, W. Kinetics of the Leaching Process of an Australian Gibbsitic Bauxite by Hydrochloric Acid. *Adv. Mater. Sci. Eng.* **2016**, *2016*, 5813542. [CrossRef]
27. Zhu, P.-W.; Zeng, W.-Q.; Xu, X.-L.; Cheng, L.-M.; Jiang, X.; Shi, Z.-L. Influence of acid leaching and calcination on iron removal of coal kaolin. *Int. J. Miner. Metall. Mater.* **2014**, *21*, 317–325. [CrossRef]
28. Li, Z.; Cao, Y.; Jiang, Y.; Han, G.; Fan, G.; Chang, L. Removal of Potassium and Iron in Low Grade Bauxite by a Calcination-Acid Leaching Process. *Minerals* **2018**, *8*, 125. [CrossRef]
29. Han, H.J.; Chen, Y.G.; Lu, J.; Xu, T.T.; Jiang, Y.H.; Bai, J.L. Investigation of removing iron from fly ash. *Adv. Mater. Res.* **2013**, *807–809*, 1194–1197. [CrossRef]
30. Li, S.; Qin, S.; Kang, L.; Liu, J.; Wang, J.; Li, Y. An Efficient Approach for Lithium and Aluminum Recovery from Coal Fly Ash by Pre-Desilication and Intensified Acid Leaching Processes. *Metals* **2017**, *7*, 272. [CrossRef]
31. Kastrinaki, G.; Lorentzou, S.; Karagiannakis, G.; Rattenbury, M.; Woodhead, J.; Konstandopoulos, A.G. Parametric synthesis study of iron based nanoparticles via aerosol spray pyrolysis route. *J. Aerosol Sci.* **2018**, *115*, 96–107. [CrossRef]
32. Zheng, J.; Liu, K.; Cai, W.; Qiao, L.; Ying, Y.; Li, W.; Yu, J.; Lin, M.; Che, S. Effect of chloride ion on crystalline phase transition of iron oxide produced by ultrasonic spray pyrolysis. *Adv. Powder Technol.* **2018**. [CrossRef]
33. Gurmen, S.; Ebin, B. Production and characterization of the nanostructured hollow iron oxide spheres and nanoparticles by aerosol route. *J. Alloys Compd.* **2010**, *492*, 585–589. [CrossRef]
34. Koo, H.Y.; Kim, J.H.; Hong, S.K.; Han, J.M.; Ko, Y.N.; Kang, Y.C.; Kang, S.H.; Cho, S.B. Characteristics of Fe powders prepared by spray pyrolysis from various types of Fe precursors as a heat pellet material. *Met. Mater. Int.* **2010**, *16*, 941–946. [CrossRef]
35. Lee, M.-S.; Ahn, J.-G.; Oh, Y.-J. Chemical Model of the $FeCl_3$-HCl-$H_2O$ Solutions at 25 °C. *Mater. Trans.* **1997**, *5639*, 1117–1133. [CrossRef]
36. Jamett, N.E.; Hernández, P.C.; Casas, J.M.; Taboada, M.E. Speciation in the Fe(III)-Cl(I)-$H_2O$ System at 298.15 K, 313.15 K, and 333.15 K (25 °C, 40 °C, and 60 °C). *Metall. Mater. Trans. B* **2018**, *49*, 451–459. [CrossRef]
37. Livenspiel, O. *Chemical Reaction Engineering*, 3rd ed.; John Wiley & Sons, Inc.: New York, NY, USA, 1999; ISBN 047125424X.
38. Tian, L.; Liu, Y.; Zhang, T.A.; Lv, G.Z.; Zhou, S.; Zhang, G.Q. Kinetics of indium dissolution from marmatite with high indium content in pressure acid leaching. *Rare Met.* **2017**, *36*, 69–76. [CrossRef]